Timelike Compton Scattering

Jakub Wagner

Theoretical Physics Department
National Centre for Nuclear Research, Warsaw

1st EIC Yellow Report Workshop at Temple University, March 19-21, 2020

So, in addition to spacelike DVCS ...

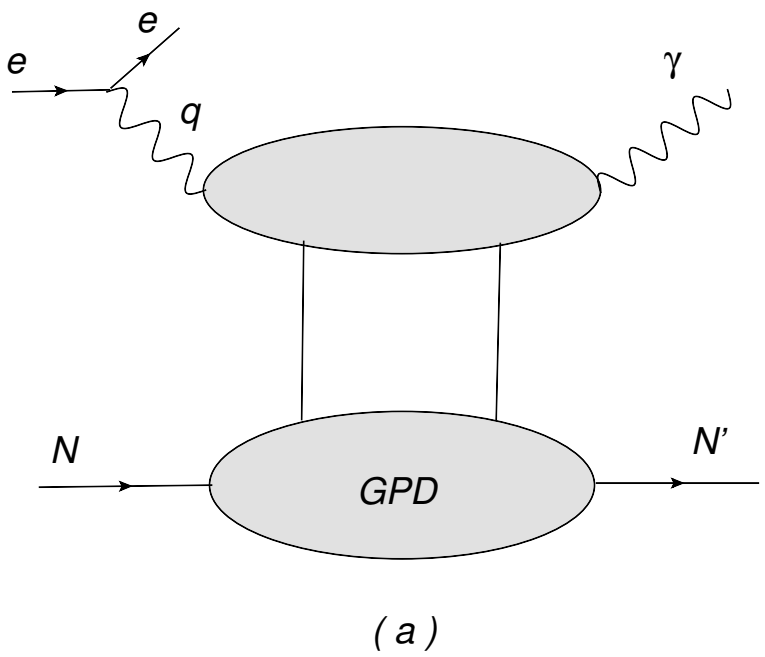

Figure: Deeply Virtual Compton Scattering (DVCS) : $lN \to l'N'\gamma$

we can also study timelike DVCS

Berger, Diehl, Pire, 2002

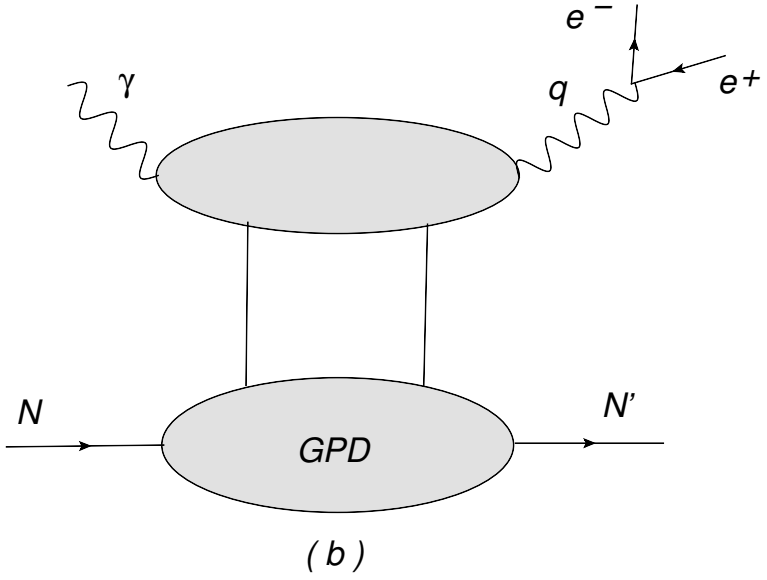

Figure: Timelike Compton Scattering (TCS): $\gamma N \to l^+ l^- N'$

Why TCS:

- universality of the GPDs
- another source for GPDs (special sensitivity on real part of GPD H),
- spacelike-timelike crossing (different analytic structure - cut in Q^2)

Coefficient functions and Compton Form Factors

CFFs are the GPD dependent quantities which enter the amplitudes. They are defined through relations:

$$\mathcal{A}^{\mu\nu}(\xi,t) = -e^2 \frac{1}{(P+P')^+}\,\bar{u}(P')\Bigg[g_T^{\mu\nu}\left(\mathcal{H}(\xi,t)\,\gamma^+ + \mathcal{E}(\xi,t)\,\frac{i\sigma^{+\rho}\Delta_\rho}{2M}\right) + i\epsilon_T^{\mu\nu}\left(\widetilde{\mathcal{H}}(\xi,t)\,\gamma^+\gamma_5 + \widetilde{\mathcal{E}}(\xi,t)\,\frac{\Delta^+\gamma_5}{2M}\right)\Bigg] u(P)\,,$$

where:

$$\begin{aligned}
\mathcal{H}(\xi,t) &= +\int_{-1}^{1} dx \left(\sum_q T^q(x,\xi)H^q(x,\xi,t) + T^g(x,\xi)H^g(x,\xi,t)\right)\\
\widetilde{\mathcal{H}}(\xi,t) &= -\int_{-1}^{1} dx \left(\sum_q \widetilde{T}^q(x,\xi)\widetilde{H}^q(x,\xi,t) + \widetilde{T}^g(x,\xi)\widetilde{H}^g(x,\xi,t)\right).
\end{aligned}$$

Spacelike vs Timelike

D.Mueller, B.Pire, L.Szymanowski, J.Wagner, Phys.Rev.D86, 2012.

Thanks to simple spacelike-to-timelike relations, we can express the timelike CFFs by the spacelike ones in the following way:

$$
\begin{aligned}
{}^T\mathcal{H} &\overset{\text{LO}}{=} {}^S\mathcal{H}^* \,, \\
{}^T\widetilde{\mathcal{H}} &\overset{\text{LO}}{=} -{}^S\widetilde{\mathcal{H}}^* \,, \\
{}^T\mathcal{H} &\overset{\text{NLO}}{=} {}^S\mathcal{H}^* - i\pi\, \mathcal{Q}^2 \frac{\partial}{\partial \mathcal{Q}^2}\, {}^S\mathcal{H}^* \,, \\
{}^T\widetilde{\mathcal{H}} &\overset{\text{NLO}}{=} -{}^S\widetilde{\mathcal{H}}^* + i\pi\, \mathcal{Q}^2 \frac{\partial}{\partial \mathcal{Q}^2}\, {}^S\widetilde{\mathcal{H}}^* \,.
\end{aligned}
$$

The corresponding relations exist for (anti-)symmetric CFFs $\mathcal{E}$ ($\widetilde{\mathcal{E}}$).

DVCS CFFs from Artificial Neural Network fit

H. Moutarde, P. Sznajder, J. Wagner, Eur.Phys.J. C79 (2019)

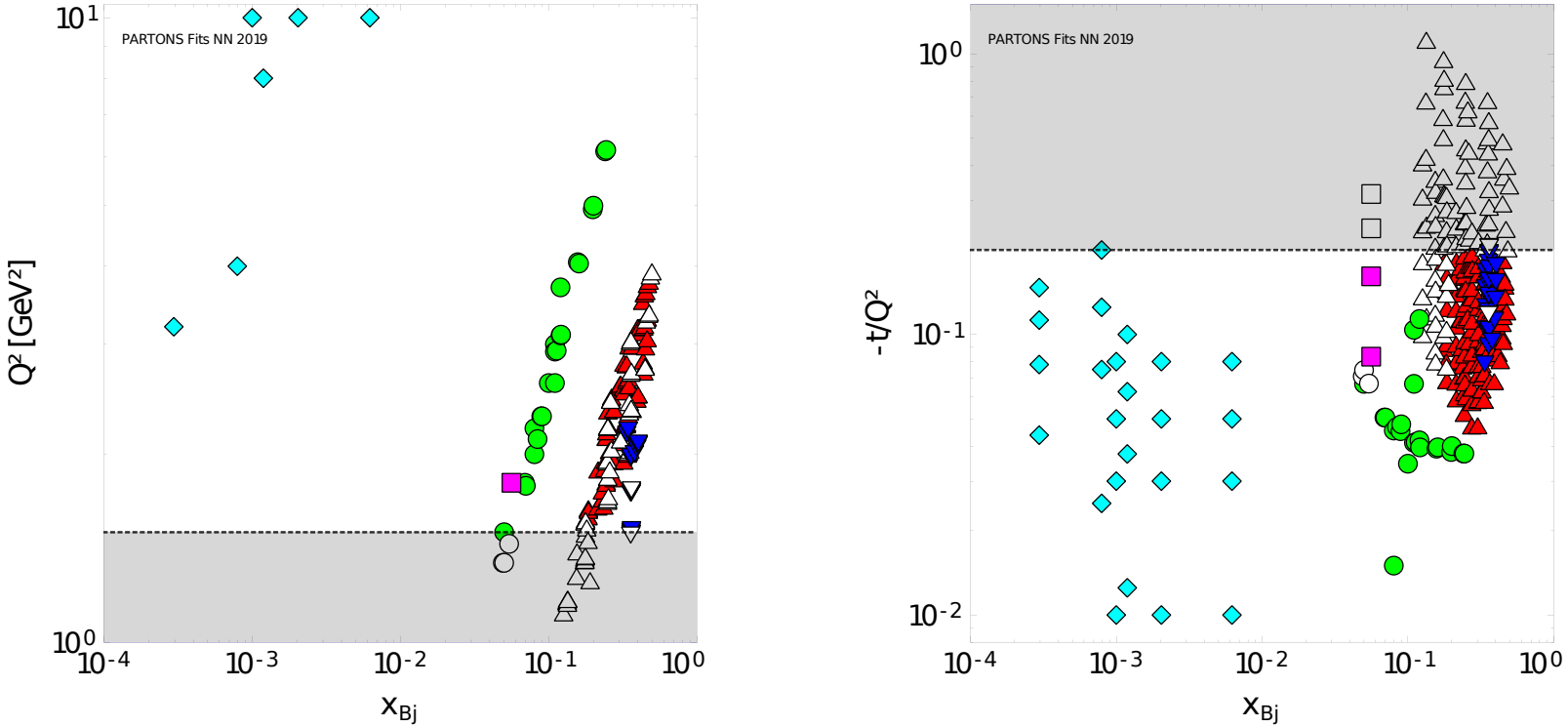

Figure: Coverage of the (x_{Bj}, Q^2) (left) and $(x_{\mathrm{Bj}}, -t/Q^2)$ (right) phase-spaces by the experimental data used in DVCS CFFs fit. The data come from the Hall A (▼, ▽), CLAS (▲, △), HERMES (●, ○), COMPASS (■, □) and HERA H1 and ZEUS (♦, ◊) experiments. The gray bands (open markers) indicate phase-space areas (experimental points) being excluded from this analysis due to the cuts.

DVCS vs TCS CFFs

O. Grocholski, H. Moutarde, B. Pire, P. Sznajder, J. Wagner, Eur.Phys.J. C80 (2020)

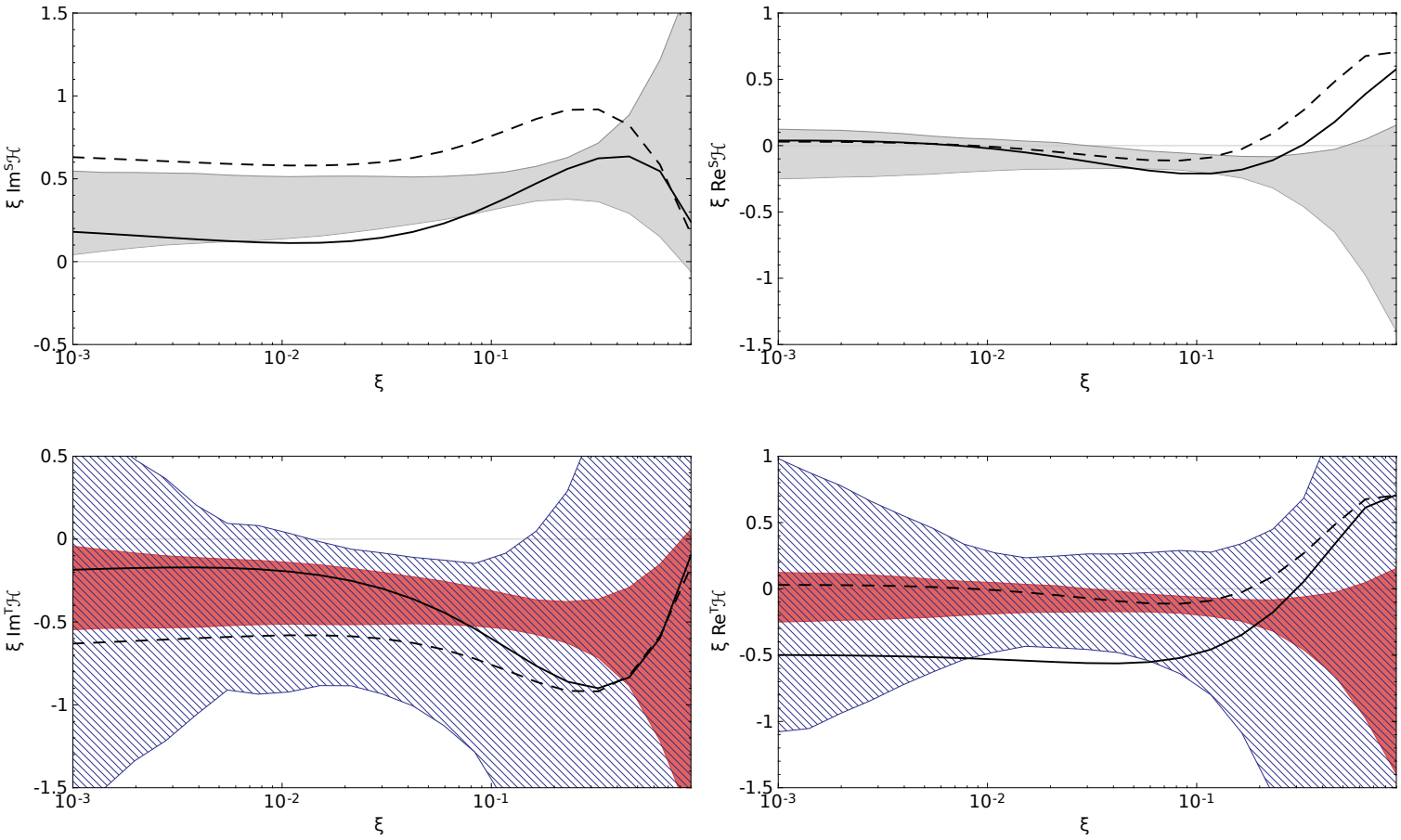

Figure: Imaginary (left) and real (right) part of DVCS (up) and TCS (down) CFF for $Q^2 = 2$ GeV^2 and $t = -0.3$ GeV^2 as a function of ξ. The shaded red (dashed blue) bands correspond to the data-driven predictions coming from the ANN global fit of DVCS data and they are evaluated using LO (NLO) spacelike-to-timelike relations. The dashed (solid) lines correspond to the GK GPD model evaluated with LO (NLO) coefficient functions.

TCS and Bethe-Heitler contribution to exclusive lepton pair photoproduction.

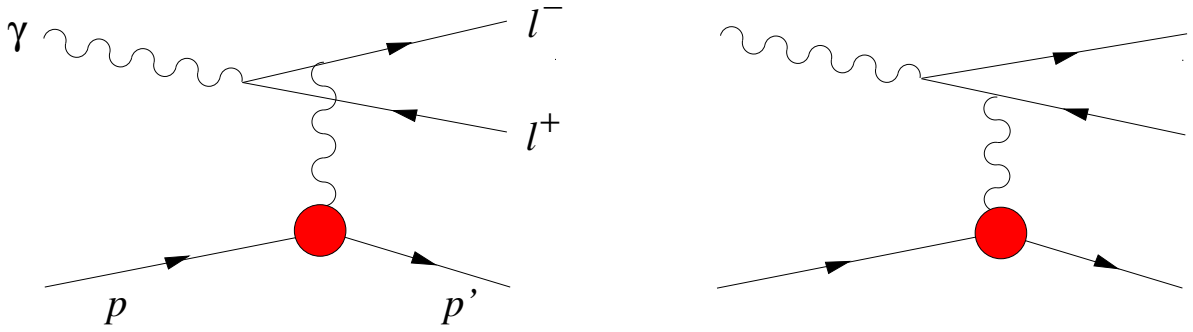

Figure: The Feynman diagrams for the Bethe-Heitler amplitude.

The cross-section for photoproduction of a lepton pair:

$$\frac{d\sigma}{dQ'^2\ dt\ d\phi\ d\cos\theta} = \frac{d\left(\sigma_{\mathrm{BH}} + \sigma_{\mathrm{TCS}} + \sigma_{\mathrm{INT}}\right)}{dQ'^2\ dt\ d\phi\ d\cos\theta}$$

TCS

Berger, Diehl, Pire, 2002

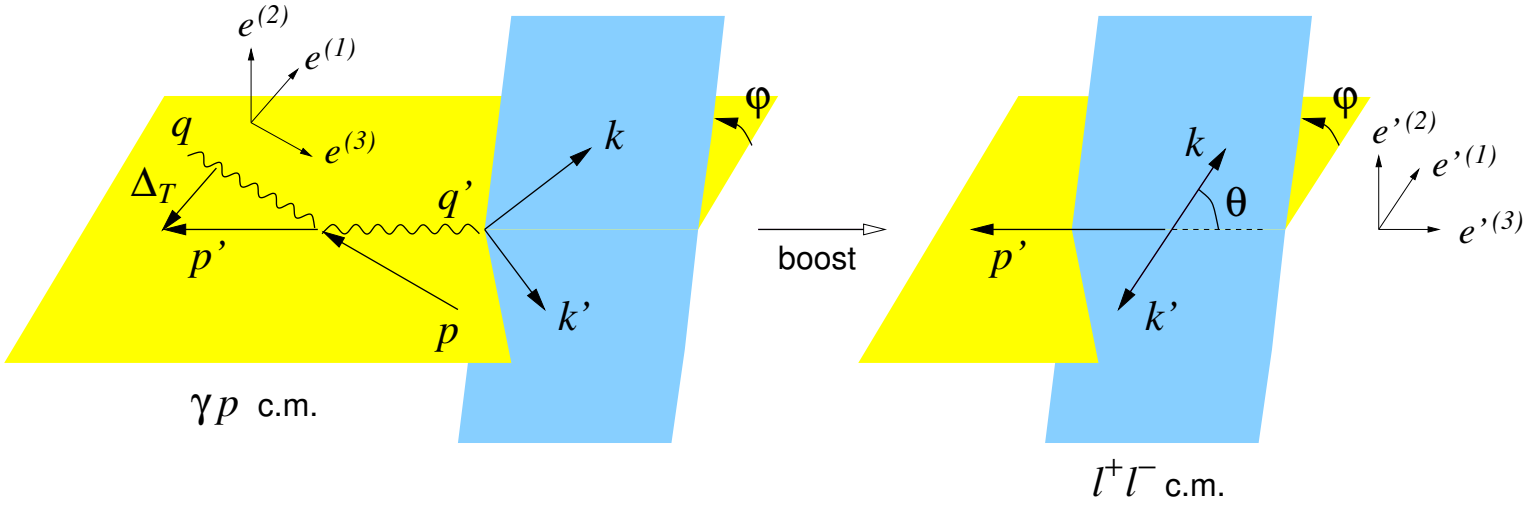

Figure: Kinematical variables and coordinate axes in the γp and $\ell^+\ell^-$ c.m. frames.

$$\frac{d\sigma}{dQ'^2\ dt\ d\phi\ d\cos\theta}$$

- Important to measure ϕ !
- BH dominates at θ close to 0 and π !

Interference

- B-H dominant for not very high energies (JLAB), at higher energies the TCS/BH ratio is bigger due to growth of the gluon and sea densities.

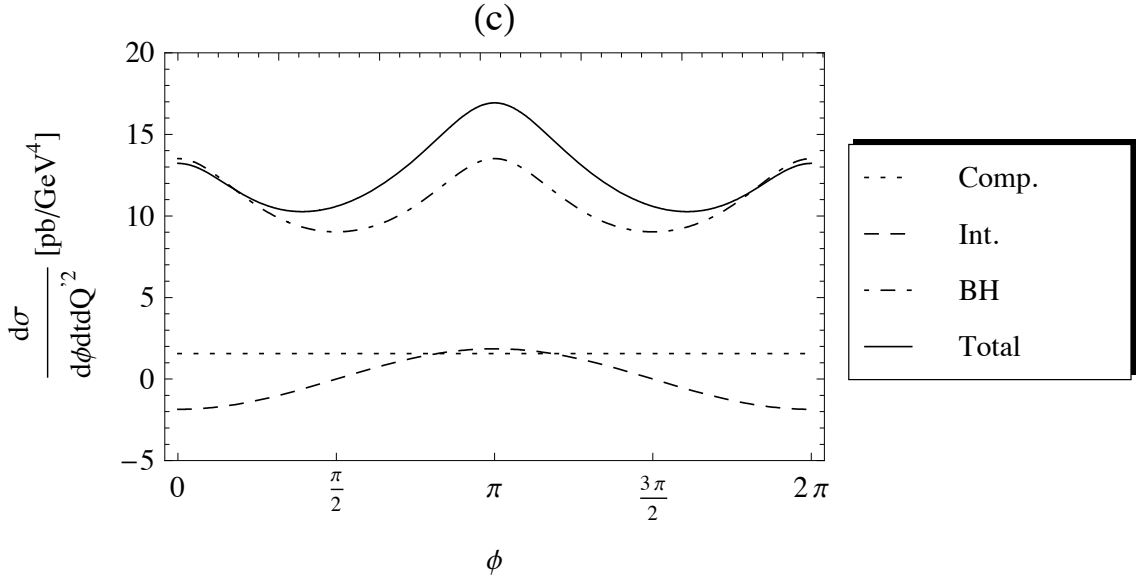

Figure: The differential cross section for $t = -0.2$ GeV^2 , $Q'^2 = 5$ GeV^2 , and integrated over $\theta \in (\pi/4, 3\pi/4)$ as a function of ϕ, for $s = 10^3$ GeV^2.

- The interference part of the cross-section for $\gamma p \to \ell^+\ell^- p$ with unpolarized protons and photons is given by:

$$\frac{d\sigma_{INT}}{dQ'^2\, dt\, d\cos\theta\, d\varphi} \sim \cos\varphi \cdot \ \mathrm{Re}\,\mathcal{H}(\xi, t) \leftarrow \text{Sensitivity to the D-term!}$$

Charge asymmetry selects interference - in DVCS one needs positron beam, here this is given by the angular dependence!

Unpolarized cross section

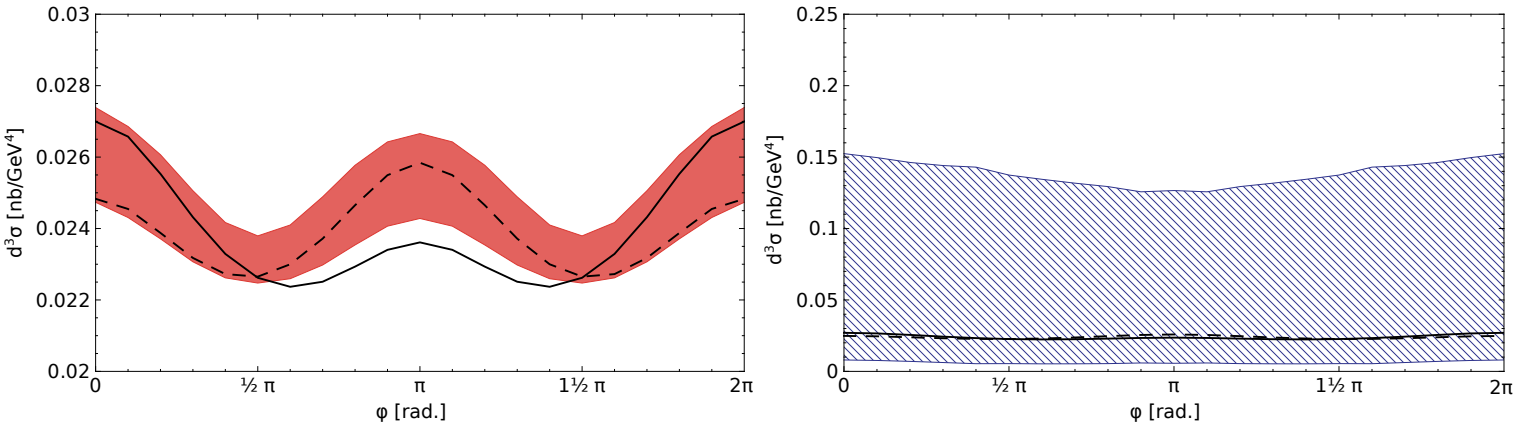

Figure: Differential TCS cross section integrated over $\theta \in (\pi/4, 3\pi/4)$ for $Q'^2 = 4$ GeV^2, $t = -0.1$ GeV^2 and the photon beam energy $E_\gamma = 10$ GeV as a function of the angle ϕ. In the left (right) panel the data-driven predictions evaluated using LO (NLO) spacelike-to-timelike relations are shown. The dashed (solid) lines correspond to the GK GPD model evaluated with LO (NLO) TCS coefficient functions (the curves are the same in both panels). Note the different scales for the upper and lower panels.

R ratio

$$R = \frac{2\int_0^{2\pi} \cos\phi \; d\phi \int_{\pi/4}^{3\pi/4} d\theta \, \frac{dS}{dQ'^2 dt d\phi d\theta}}{\int_0^{2\pi} d\phi \int_{\pi/4}^{3\pi/4} d\theta \, \frac{dS}{dQ'^2 dt d\phi d\theta}} \, ,$$

where S is the weighted cross section :

$$\frac{dS}{dQ'^2 dt d\phi d\theta} = \frac{L(\theta,\phi)}{L_0(\theta)} \frac{d\sigma}{dQ'^2 dt d\phi d\theta} \, ,$$

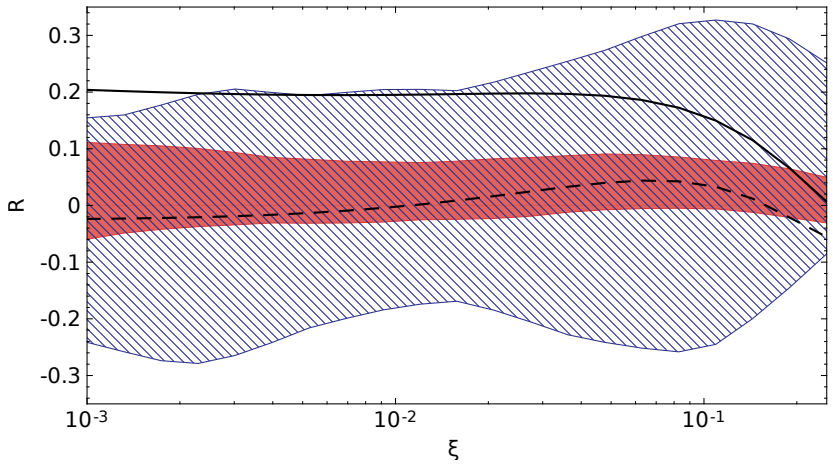

Figure: Ratio R evaluated with LO and NLO spacelike-to-timelike relations for $Q'^2 = 4$ GeV^2, $t = -0.35$ GeV^2 as a function of ξ.

Circular asymmetry

The photon beam circular polarization asymmetry:

$$A_{CU} = \frac{\sigma^+ - \sigma^-}{\sigma^+ + \sigma^-} \sim Im(H)$$

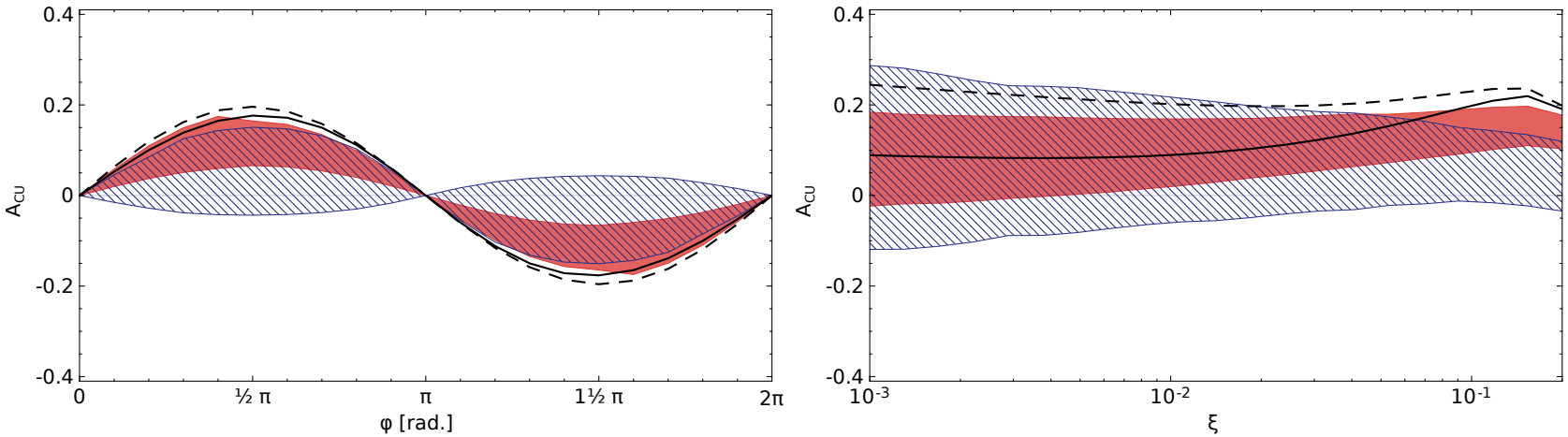

Figure: Circular asymmetry A_{CU} evaluated with LO and NLO spacelike-to-timelike relations for $Q'^2 = 4$ GeV^2, $t = -0.1$ GeV^2 and (left) $E_\gamma = 10$ GeV as a function of ϕ (right) and $\phi = \pi/2$ as a function of ξ. The cross sections used to evaluate the asymmetry are integrated over $\theta \in (\pi/4, 3\pi/4)$.

Transverse target asymmetry

$$\frac{d\sigma^{\rm tpol}_{\rm INT}}{dQ'^2 d(\cos\theta) d\phi dt d\varphi_S} \sim \sin\varphi_S \Im\Big[\mathcal{H} - \frac{\xi^2}{1-\xi^2}\mathcal{E} + \widetilde{\mathcal{H}} + \frac{t}{4M^2}\widetilde{\mathcal{E}}\Big]. \qquad (1)$$

The transverse spin asymmetry:

$$A_{UT}(\varphi_S) = \frac{\sigma(\varphi_S) - \sigma(\varphi_S - \pi)}{\sigma(\varphi_S) + \sigma(\varphi_S - \pi)}\,, \qquad (2)$$

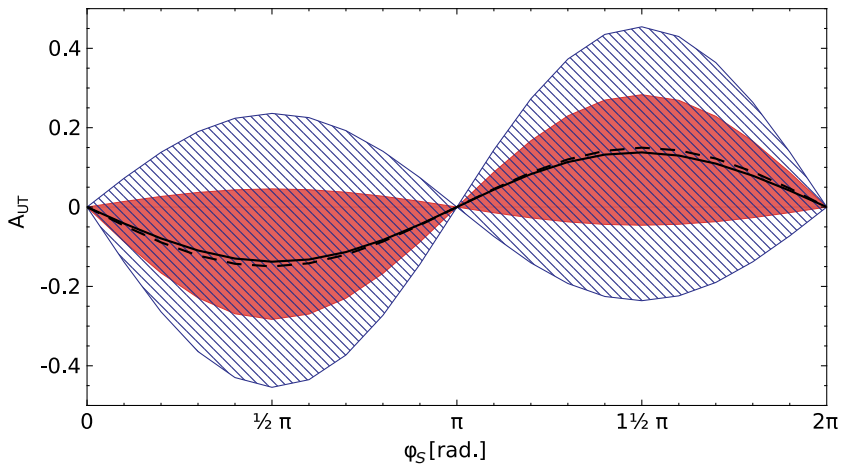

Figure: Transverse target spin asymmetry A_{UT} evaluated with LO and NLO spacelike-to-timelike relations for $Q'^2 = 4$ GeV^2, $t = t_0$ and $E_\gamma = 10$ GeV as a function of φ_S. The cross sections used to evaluate the asymmetry are integrated over $\theta \in (\pi/4, 3\pi/4)$.

Experimental status

Rafayel Paremuzyan PhD thesis

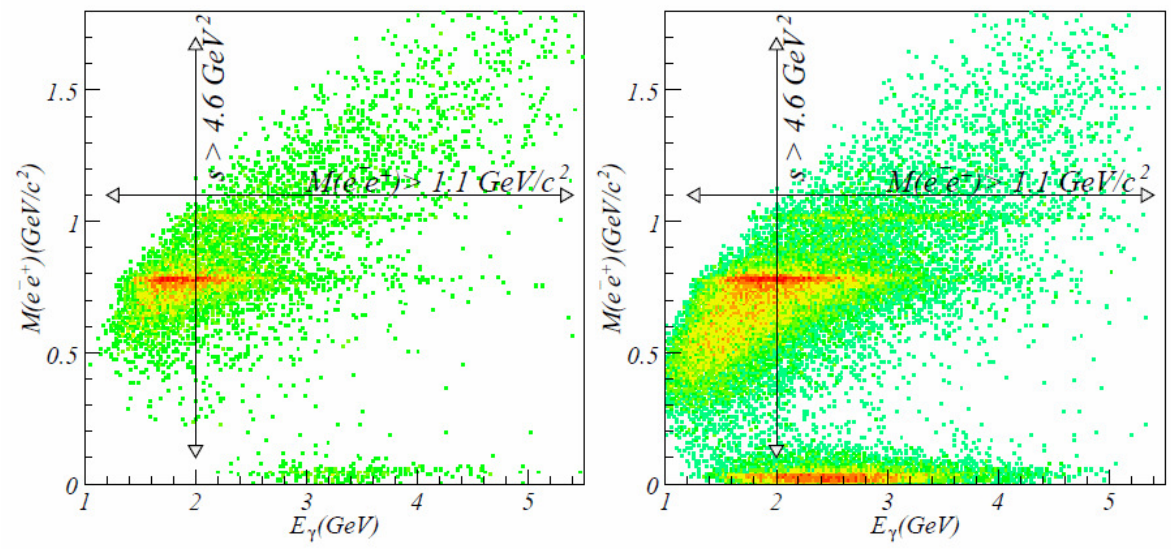

Figure: e^+e^- invariant mass distribution vs quasi-real photon energy. For TCS analysis $M(e^+e^-) > 1.1\,\mathrm{GeV}$ and $s_{\gamma p} > 4.6\,\mathrm{GeV}^2$ regions are chosen. Left graph represents e1-6 data set, right one is from e1f data set.

Experimental status

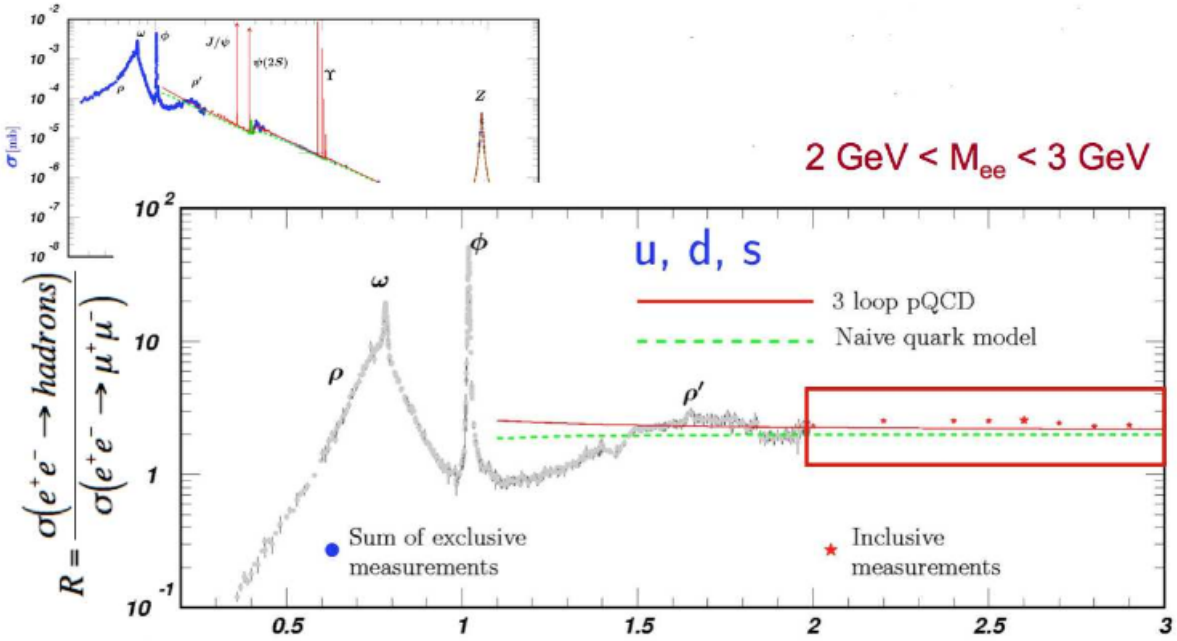

FIG. 4: Measurements of e^+e^- annihilation into hadrons show a resonance-free window between the ρ' and the J/ψ, which is ideal for TCS studies at 12 GeV.

- CLAS - E12-12-001 : First preliminary results presented at Light Cone 2019, Pierre Chatagnon
- UPC's ?

Summary

- TCS is complementary measurement to DVCS, cleanest way to test universality of GPDs,
- Timelike-spacelike relations at LO/NLO gives us tools to use TCS data in DVCS CFF fits, with special sensitivity to Q^2 dependence,
- First data-driven and model-free predictions for TCS using global DVCS data (Grocholski, Moutarde, Pire, Sznajder, JW)
- TCS measured at JLAB 6 GeV (Rafayel Paremuzyan), but much richer and more interesting kinematical region available after upgrade to 12 GeV (P.Chatagnon, S.Niccolai)
- Numerical studies of TCS by Boer, Guidal and Vanderhaeghen
- Impact studies for JLAB by M.Boer
- Possible also in UPCs in LHC Charlotte van Hulse - TCS on nuclei needed for asymmetric collisions

What next:

- **PARTONS v2** (http://partons.cea.fr) TCS implemented: CFFs, cross sections, observables at LO/NLO,
- ready for the more detailed studies and simulations for EIC

We can replace dilepton (= TCS) by diphoton; i.e. $Q'^2 \to M^2_{\gamma\gamma}$

Hard photo- and electroproduction of a diphoton with a large invariant mass

A. Pedrak, B. Pire, L. Szymanowski, JW, Phys.Rev. D96

A. Pedrak, B. Pire, L. Szymanowski, JW, arXiv:2003.03263

$$\gamma(q,\epsilon) + N(p_1,s_1) \to \gamma(k_1,\epsilon_1) + \gamma(k_2,\epsilon_2) + N'(p_2,s_2)$$

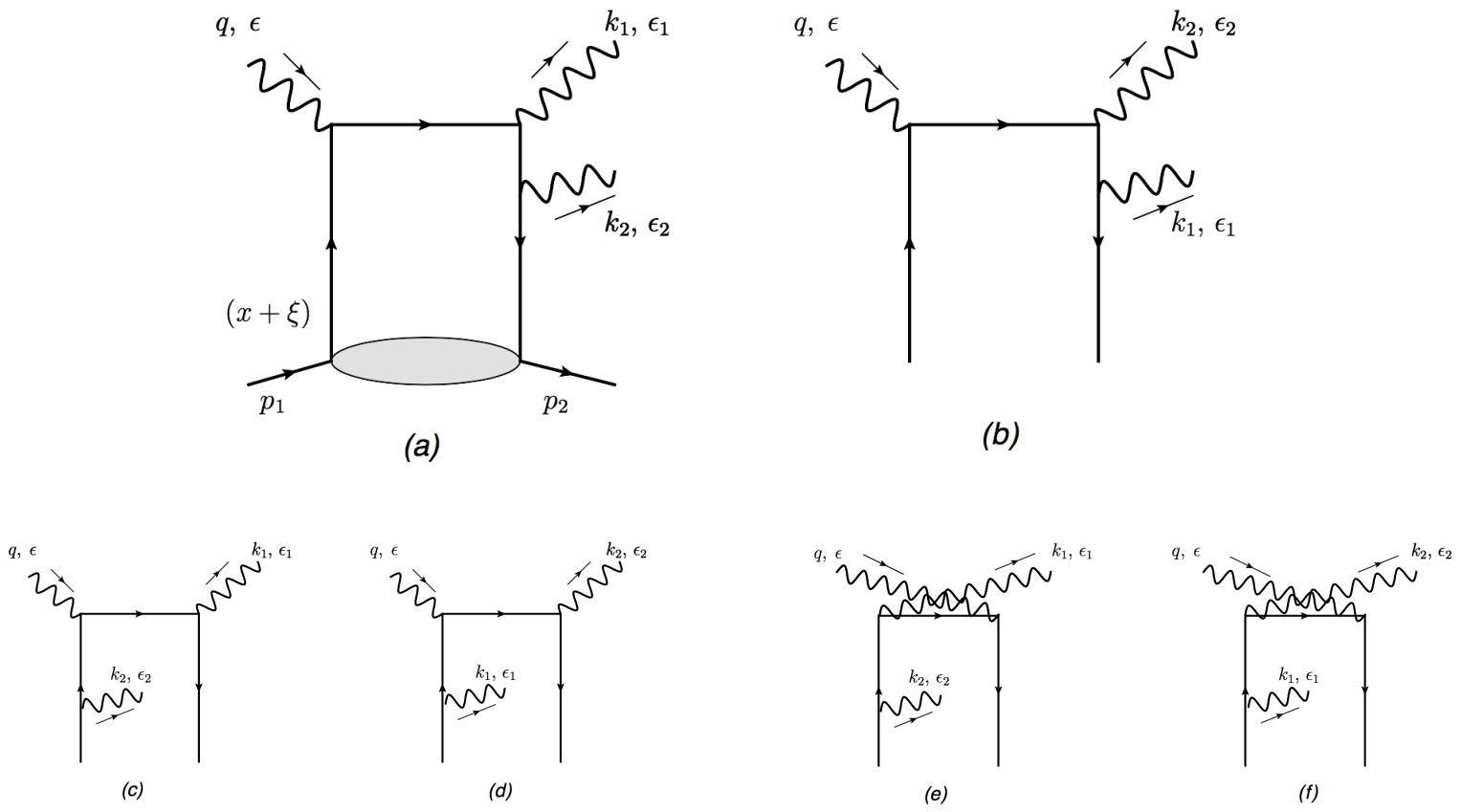

Figure: Feynman diagrams contributing to the coefficient function of the process $\gamma N \to \gamma\gamma N'$

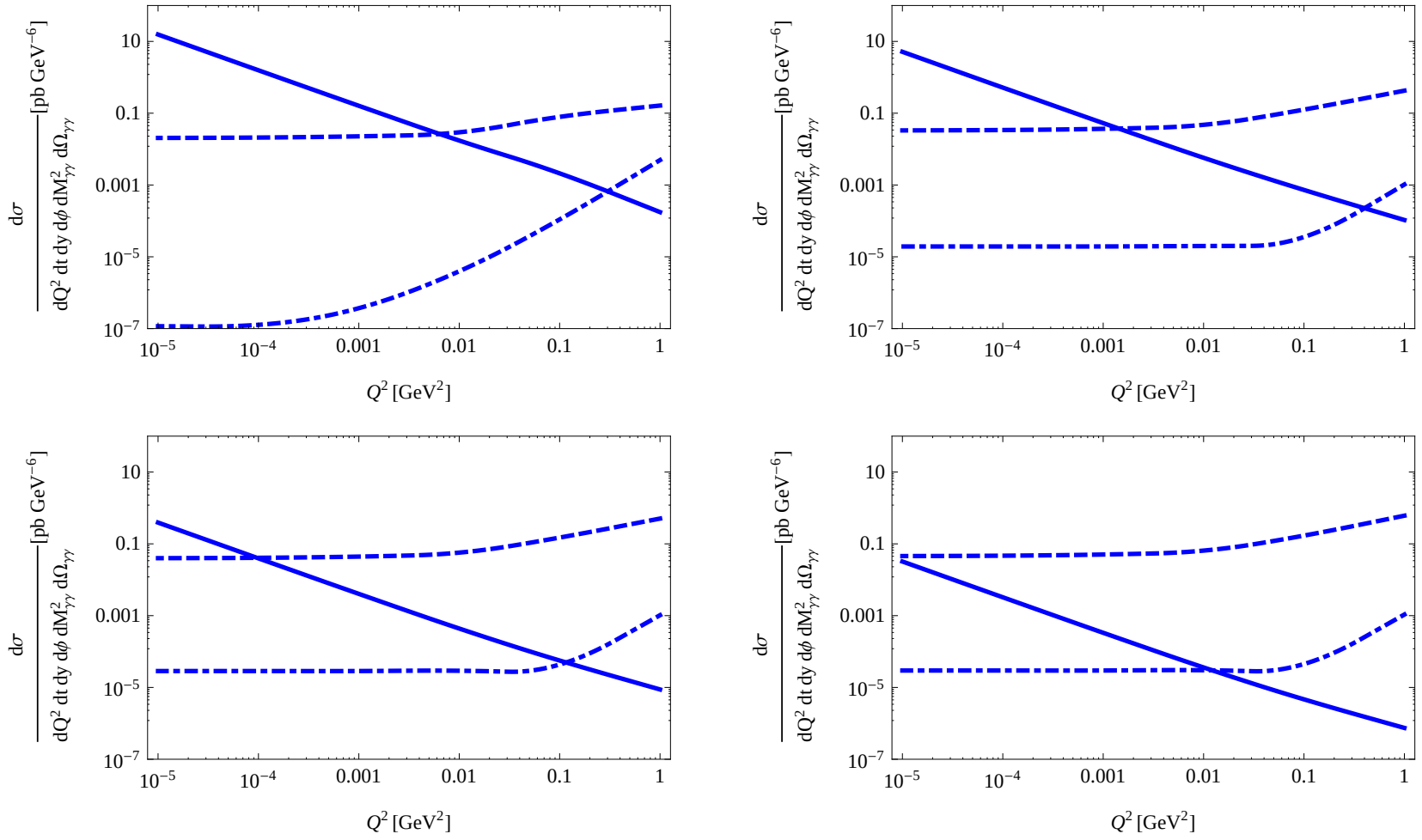

Figure: From left to right and from top to bottom: $s = 20$ GeV^2, $s = 100$ GeV^2, $s = 1000$ GeV^2 and $s = 10000$ GeV^2 at the kinematical point $M^2_{\gamma\gamma} = 3$ GeV^2, $\theta = 3\pi/8$, $\phi_{\gamma\gamma} = 0$, $y = 0.6$ as a function of Q^2. The QCD process (solid curve) dominates at very low Q^2, the single Bethe-Heitler process (dashed curve) dominates at higher Q^2 while the double Bethe-Heitler process (dotted curve) is always subdominant.